American Mineralogist, Volume 76, pages 713–727, 1991

Relative scales of thermal- and fluid infiltration-driven metamorphism in fold nappes, New England, U.S.A.

DANIEL E. BARNETT, C. PAGE CHAMBERLAIN

Department of Earth Sciences, Dartmouth College, Hanover, New Hampshire 03755, U.S.A.

ABSTRACT

Metamorphism of the Waits River Formation (WRF) was studied using petrologic and stable isotopic methods in order to determine the relative importance and scales of thermal perturbations and fluid infiltration during folding and regional metamorphism at mid-crustal levels. Metamorphism of the WRF involved the growth of biotite and tremolite at the expense of muscovite and dolomite. Reaction progress in synclines is enhanced relative to anticlines and involved considerable devolatilization of CO_2. The C-O-H fluid in equilibrium with the WRF during metamorphism was an H_2O-rich binary H_2O-CO_2 mixture. Petrologic considerations yield fluid/rock ratios of between 0.01 and 1.07 in O equivalents with higher fluid/rock ratios in samples containing tremolite.

Comparison of observed values of $\delta^{13}C_{carb}$ with calculated values based on Rayleigh distillation shows that Rayleigh distillation has affected the isotopic composition of C in carbonate. The calculations indicate that either some samples were subjected to infiltration of fluids relatively depleted in ^{13}C or that heterogeneities in $\delta^{13}C_{carb}$ existed in the protoliths.

Calculated shifts in $\delta^{18}O_{carb}$ based on lever-rule effects and Rayleigh distillation are smaller than, and in some cases in the opposite direction of, observed shifts based on a protolith value of $\delta^{18}O_{carb} = 20‰$. Infiltration of an O-bearing fluid depleted in ^{18}O relative to the calc-silicates is necessary to explain the shifts in $\delta^{18}O_{carb}$ observed in these rocks. Isotopic considerations yield fluid/rock ratios in qualitative agreement with those calculated through petrologic considerations.

Mass balance considerations show that the amount of hydrous fluid necessary for fluid-present metamorphism in the calc-silicate unit could be derived from dehydration of the immediately adjacent amphibolites and pelitic schists.

Based on the distribution of metamorphic isograds and the extent of fluid/rock interaction, it is concluded that the differences in metamorphic grade between fold sets are the result of thermal perturbations on a scale of tens of square kilometers. The differences in metamorphic grade within individual folds are the result of differences in the amount of fluid infiltration that varies over a distance of tens or hundreds of meters.

INTRODUCTION

Two fundamentally different mechanisms by which regional metamorphism occurs have been proposed in the recent literature. One model holds that regional metamorphism occurs in response to thermal perturbations resulting from crustal deformation (Sleep, 1979; England and Thompson, 1984; Allen and Chamberlain, 1989), igneous intrusion (Lux et al., 1986), or both. Evidence for regional metamorphism in response to thermal perturbations includes (1) the spatial relationship between increased metamorphic grade and large granitic batholiths (Lux et al., 1986), (2) the spatial relationship between metamorphic grade and large scale folds and faults (Fisher, 1980; Spear et al., 1984; Chamberlain, 1986; Chamberlain et al., 1989), and (3) the relationship between pressure-temperature-time paths and regional deformation events (Spear et al., 1984; Selverstone et al., 1984).

The other model holds that regional metamorphism occurs in response to the infiltration of chemically reactive fluids that drive devolatilization reactions (Rumble et al., 1982; Tracy et al., 1983; Ferry, 1984, 1987). The evidence for regional metamorphism occurring in response to fluid infiltration comes from both petrologic and stable isotopic studies. Petrologic studies have shown that the composition of the fluid phase produced by prograde metamorphism of many rocks is out of chemical equilibrium with the solid phases present (Ferry, 1983, 1987; Tracy et al., 1983; Mohr, 1985; see Rice and Ferry, 1982, Table 2 for earlier references). In such cases, it is assumed that the rock is infiltrated by a fluid out of chemical equilibrium with the mineral assemblage and reaction proceeds until the equilibrium fluid composition is reached.

Stable isotopic studies have shown that isotopic shifts commonly correlate with increasing metamorphic grade (Rumble et al., 1982; Tracy et al., 1983; Graham et al.,

0003–004X/91/0506–0713$02.00

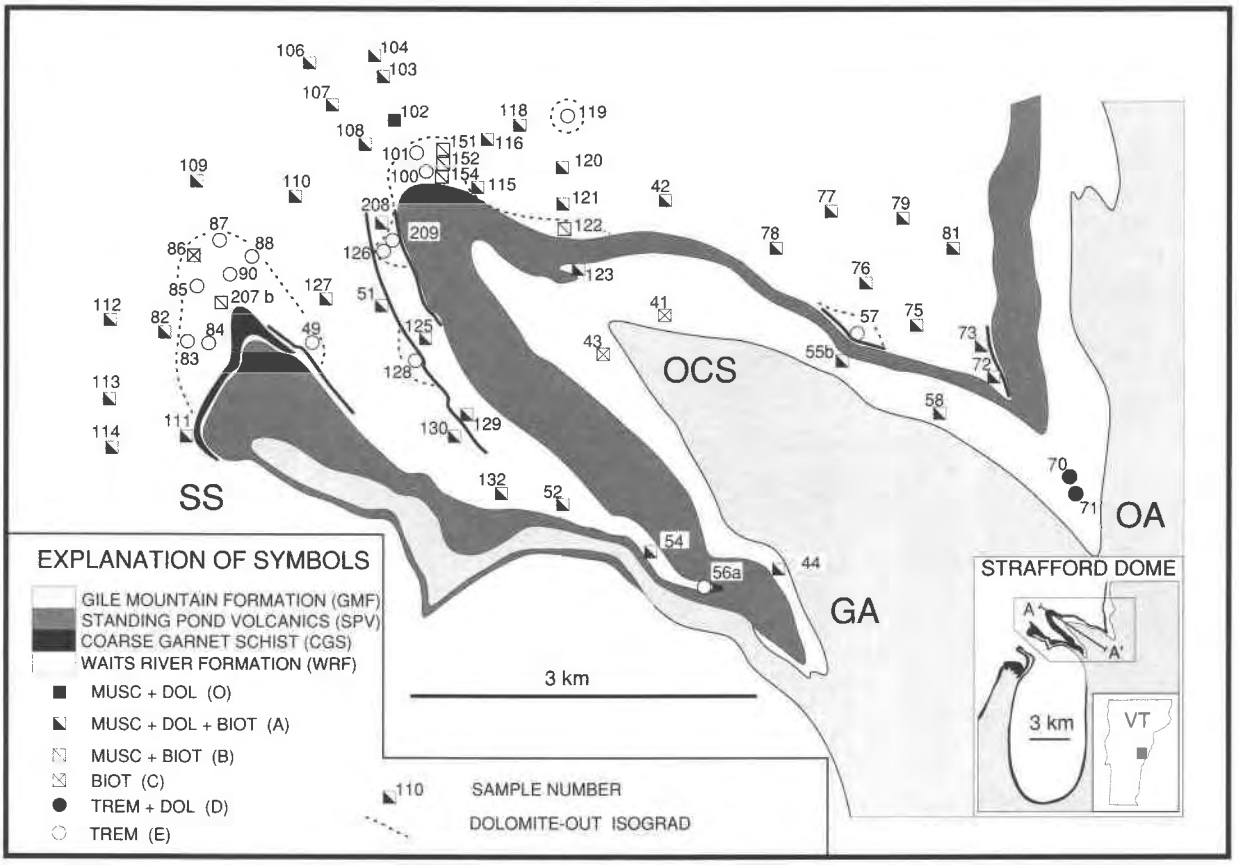

Fig. 1. Geologic map of the Strafford, Vermont, area showing the locations of outcrops discussed in text, the distribution of metamorphic assemblages, and the dolomite-out isograd. Heavy black lines are thin beds of coarse garnet schist. Line A-A′ in inset gives the location of the cross section in Figure 2. Geology after Doll (1944) and White and Jahns (1950).

1983; Hoernes and Hoffer, 1985; Wickham and Taylor, 1985; Chamberlain and Rumble, 1988) and that minerals and rocks of different bulk compositions may be isotopically homogenized over a wide geographic area (Taylor et al., 1963; Wickham and Taylor, 1985). These isotopic features are thought to result from fluid infiltration during metamorphism.

It is evident that both the process of fluid-driven and thermally driven metamorphism occur during regional metamorphism. However, the questions that remain are (1) in what geological settings do these different processes dominate; and (2) over what time and length scale do these different processes operate. The answers to these difficult and important questions will, in part, come from an increased number of case studies of regional metamorphic terranes.

The purpose of this study is to compare the roles of thermal perturbations and fluid infiltration during metamorphism of large scale folds in a medium pressure regional metamorphic terrane. We undertook this study because geophysical studies (Sleep, 1979) and petrologic studies (Fisher, 1980; Chamberlain, 1986) show that large scale folding can significantly affect the metamorphic history of a terrane. If folding is sufficiently rapid, isotherms will be displaced. The subsequent relaxation of isotherms will result in cooling in anticlinal folds and heating in synclinal folds (Sleep, 1979). This process of folding and relaxing of isotherms has been suggested as an explanation for the metamorphic histories observed in two different metamorphic terranes in New England (Fisher, 1980; Chamberlain, 1986). It is possible, however, that the different metamorphic histories observed in these fold sets could result from fluid-driven rather than thermally driven metamorphism. To date, no studies have examined the effect of fluids in these folded terranes.

In this study, we employ petrologic and stable isotopic techniques in order to examine the regional metamorphism of calcareous sediments in east central Vermont. We chose this area because it contains large scale fold nappes that consist of calcareous metasediments interbedded with pelitic metasediments. Calcareous metasediments record easily retrievable petrologic and stable isotopic information about fluid/rock interaction while pelitic metasediments record thermal perturbations in a chemical system that is relatively unaffected by fluid composition. Our work shows that in the calcareous

metasediments, thermal heterogeneities are the dominant driving force of metamorphism over areas of tens of square kilometers. However, over areas of hundreds of square meters, there is evidence that fluid-driven metamorphism is important.

Geologic setting

The study area is located in the Strafford Quadrangle in east-central Vermont (Fig. 1). Detailed stratigraphic and structural investigations in the area were conducted by Doll (1944) and by White and Jahns (1950). Howard (1969) provides an overview of earlier geologic studies in the Strafford and surrounding areas.

Stratigraphy

The strata in the study area include, from oldest to youngest, the Waits River Formation, the Standing Pond Volcanics, and the Gile Mountain Formation. The Waits River Formation (WRF) consists of thinly interbedded calcareous metasandstones and quartz mica schists. The calcareous metasandstones contain minor micaceous minerals and the quartz mica schists are locally garnetiferous. In the Strafford area, the Standing Pond Volcanics (SPV) consist of black to gray amphibolite. A coarse-grained aluminous garnet schist termed the coarse garnet schist (CGS) occurs at places between the SPV and WRF and within the WRF (Fig. 1). The Gile Mountain Formation (GMF) consists of interbedded quartzitic schists and micaceous quartzites.

Hueber et al. (1990) have assigned a Siluro-Devonian stratigraphic age to these metasediments based on correlative fossiliferous strata in southern Quebec. The area underwent deformation and regional metamorphism during the Devonian Acadian Orogeny.

Structure

The structure of east-central Vermont, with special attention to the area of this study, was examined by White and Jahns (1950). The entire package of sediments has been isoclinally folded to form the four major fold nappes at the north end of the Strafford dome (Fig. 1). These include, from north to south, the Orange anticline (OA), the Old City syncline (OCS), the Grannyhand anticline (GA), and the Strafford syncline (SS). These fold nappes have been refolded by the uplift of the Strafford dome (Fig. 2), so that the fold axes of the folds at the north end of the dome trend north-northeast and plunge about 30° north (White and Jahns, 1950).

Because of the uplift of the Strafford dome, the mirror images of these folds can be seen across the septum of WRF in the northwest corner of the dome. Here the fold axes trend about due west and plunge more steeply (White and Jahns, 1950).

Metamorphism of pelitic rocks

Details of petrologic studies of the pelitic schists in the WRF and GMF will be reported elsewhere (Barnett and Chamberlain, in preparation). Here were present conclusions relevant to this study. (1) Peak metamorphic temperatures determined by garnet-biotite geothermometry on 14 samples range from 475 to 583 °C and average 525 °C. Peak metamorphic temperatures increase from north to south and from east to west within the fold nappes. Approximate peak metamorphic isotherms are shown in Figure 2. Pressures determined from garnet-feldspar solid solutions range from 4.7 to 8.6 kbar and average 6.2 kbar. Pressure determinations are stongly temperature dependent. (2) Prograde metamorphism occurred to a small extent before formation of the fold nappes and to a large extent during and after formation of the fold nappes. (3) Folding was sufficiently rapid that steady state isothermal surfaces were perturbed. (4) Reaction progress in the Old City and Strafford synclines was enhanced relative to that in the Orange and Grannyhand anticlines because of this folding and subsequent relaxation of isothermal surfaces.

These conclusions are in agreement with previous studies of metamorphism in east Vermont (Lyons, 1955; Rosenfeld, 1968; Fisher, 1980; Hepburn et al., 1984).

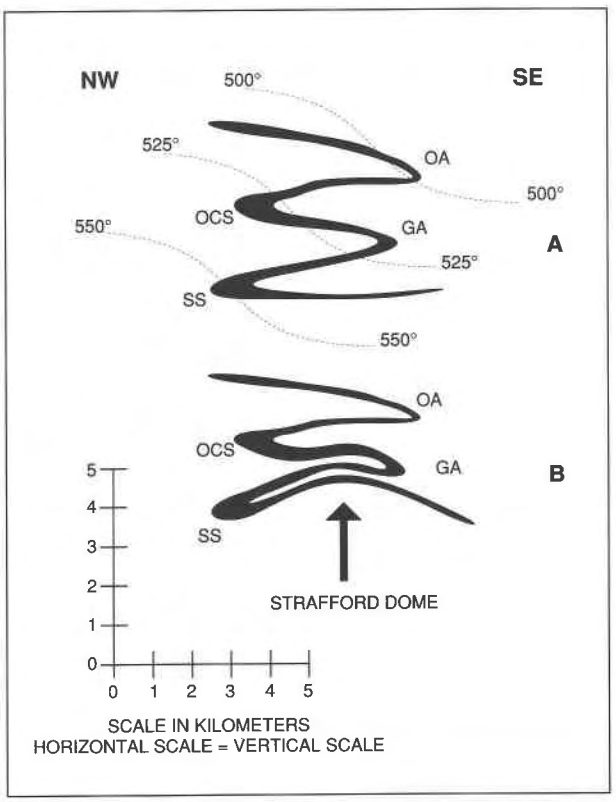

Fig. 2. Vertical cross sections through line A-A′ in inset of Figure 1. (**A**) Prior to, and (**B**) subsequent to uplift of the Strafford dome. Approximate location of isotherms after isoclinal folding shown in **A**. Vertical scale = horizontal scale.

Analytical methods

Samples were cut into approximately 100 cm^3 blocks from which was cut a tablet for a 3 × 5 cm thin section for modal mineral analysis. The rest of each sample was

Table 1. Representative microprobe analyses

WR-73	Muscovite	Biotite	Feldspar	Calcite	Dolomite
SiO_2	46.30	37.97	46.97	—	—
TiO_2	1.26	1.44	—	—	—
Al_2O_3	32.82	18.77	34.08	—	—
FeO	0.98	12.29	0.05	1.38	7.59
MgO	1.30	14.27	0.00	1.74	15.79
MnO	0.00	0.03	—	0.41	0.48
CaO	0.06	0.17	16.45	50.12	29.40
Na_2O	0.56	0.20	1.80	—	—
K_2O	10.76	9.35	0.02	—	—
Total	94.04	94.49	99.37	53.65	53.26
Si	3.13	2.80	2.16	—	—
Ti	0.06	0.08	—	—	—
Al	2.61	1.63	1.85	—	—
Fe	0.06	0.76	0.00	0.02	0.10
Mg	0.13	1.57	0.00	0.04	0.38
Mn	0.00	0.00	—	0.01	0.01
Ca	0.00	0.01	0.81	0.93	0.51
Na	0.07	0.03	0.16	—	—
K	0.93	0.88	0.00	—	—

WR-83a	Tremolite	Biotite	Feldspar	Calcite
SiO_2	54.28	39.32	57.72	—
TiO_2	0.17	1.11	—	—
Al_2O_3	4.24	17.44	27.17	—
FeO	4.23	6.47	0.02	0.62
MgO	20.40	19.51	0.00	1.63
MnO	0.13	0.03	—	0.27
CaO	12.84	0.04	8.27	51.35
Na_2O	0.42	0.09	6.45	—
K_2O	0.16	10.30	0.05	—
Total	96.87	94.31	99.68	52.87
Si	7.58	2.84	2.58	—
Ti	0.02	0.06	—	—
Al	0.70	1.48	1.43	—
Fe	0.49	0.15	0.00	0.01
Mg	4.25	2.10	0.00	0.04
Mn	0.01	0.00	—	0.00
Ca	1.92	0.00	0.40	0.95
Na	0.11	0.01	0.56	—
K	0.03	0.95	0.00	—

Note: Stoichiometries as follows: tremolite = cations/23 O atoms; micas = cations/11 O atoms; feldspars = cations/8 O atoms; carbonates = cations/1 O atom.

crushed and ground to sand-sized particles. One split of the sample was ground to a fine powder for 3 min in an automatic mortar and the other split was saved for mineral separations.

Mineral modes were determined by point counts of 1000 to 2000 points in thin sections. Mineral compositions were determined on the Cameca electron microprobe at Harvard University using natural and synthetic silicate, oxide, and carbonate standards. Chemical compositions were determined from X-ray data following Bence and Albee (1968). All analyses were collected using a 15 kV accelerating voltage and a beam current of 15 nA. Whole rock chemical analyses were performed on a fraction of homogenized powder from 12 samples by X-Ray Assay Labs in Dons Mills, Ontario.

Isotopic compositions of C and O in carbonate from samples of Waits River Formation were determined by reacting 30 mg of powdered whole rock samples using the H_3PO_4 method of McCrea (1950). The carbonate in the samples analyzed was either calcite or a mixture of calcite and dolomite. Using timed experiments, we were unable to distinguish between the CO_2 liberated by calcite and dolomite in samples that contained both carbonates. All samples were reacted overnight. Because the isotopic fractionation of C and O between calcite and dolomite is small at metamorphic temperatures (Friedman and O'Neil, 1977), and because the amount of dolomite present in these samples is small, the presence of two carbonates in measured samples does not seriously affect the conclusions presented in this paper.

Quartz was separated from the whole rock using heavy liquids and a magnetic separator. Samples were treated with HCl, HF, and NaOH and dried before analysis. O isotopes were measured for quartz using the BrF_5 technique of Clayton and Meyeda (1963) and O extraction line located at Dartmouth College.

O and C isotope ratios were measured using the Delta E Finnigan mass spectrometer at Dartmouth College. For carbonates, analyses were reproducible to better than ± 0.1 per mil. For quartz, analyses were reproducible to better than ± 0.2 per mil. C and O isotopic compositions are reported relative to PDB and SMOW, respectively.

Petrologic study

Mineral assemblages

Six mineral assemblages are recognized in the calcareous metasandstones of the Waits River Formation in the study area. The assemblages are distinguished by the presence or absence of dolomite, muscovite, biotite, and calcic amphibole. All assemblages contain quartz + plagioclase feldspar + calcite + graphite ± minor chlorite, ilmenite, and iron sulfide. Assemblage O contains dolomite and muscovite. Assemblage A contains dolomite, muscovite, and biotite, while assemblage B contains muscovite and biotite without dolomite. Assemblage D contains dolomite, biotite, and calcic amphibole while assemblage E contains calcic amphibole and biotite without dolomite. Assemblage C contains biotite with no muscovite, dolomite, or calcic amphibole.

The locations of samples containing assemblages O and A–E shown in Figure 1. Assemblages lacking dolomite are for the most part located in fold hinges near the Standing Pond Volcanics, but also occur in a few locations in fold limbs. Of the four dolomite absent samples located in fold limbs, two are adjacent to the Standing Pond Volcanics and one is adjacent to a mapped occurrence of the Coarse Garnet Schist. The spatial relationship between dolomite out assemblages and these two units is addressed in a later section.

Mineral compositions

In order to quantify the reactions by which metamorphism occurred, and to assess the temperature and fluid composition during metamorphism, compositional data on micas, feldspars, amphiboles, and carbonates were collected from 28 samples of calcareous metasandstones from the Waits River Formation. Representative analyses are presented in Table 1.

Carbonate. Two carbonates, calcite and dolomite, are present in the study area. Both minerals contain significant amounts of Fe, and dolomite contains considerable Mn. Mg is present in greater quantity than Fe in both carbonates. Calcite coexisting with dolomite does not necessarily contain greater noncalcium components than calcite from single carbonate samples. Neither siderite nor magnesite were observed in any sample.

Feldspar. Plagioclase feldspar compositions in samples from the study area range from An_{18} to An_{90}. Wide compositional variation is recorded within a single polished section and even within single grains. Both zoned and unzoned feldspars are present in most samples. Feldspars in the study area have uniformly low K content and nonternary feldspar components are negligible in all analyzed samples.

Amphibole and mica. We have adopted the method of Bragg (1937) and later workers (Bragg and Claringbull, 1965; Thompson, 1979, 1981, 1982a; Thompson et al., 1982) in describing the compositions of amphibole and mica in terms of a single additive compositional component modified by a set of linearly independent exchange components. Thompson et al. (1982) show that coupled substitutions, e.g., $Al_2Si_{-1}Mg_{-1}$ (tk), can have a significant effect on the modal mineralogy of a rock during metamorphism, but simple cation substitutions, e.g., $FeMg_{-1}$, generally cannot. Analysis of compositional data of minerals in terms of additive and exchange components provides a simple way of determining which of the exchange components that represent coupled substitutions are likely to exert an important influence on the mineral assemblage during metamorphism. In this analysis, all Fe is assumed to be divalent and amphibole and mica are assumed to be stiochiometrically hydrated.

For calcic amphibole, the components used are the same as in Thompson (1981). The additive component is end-member tremolite, which is modified by simple cation exchange components plus the coupled substitutions $Al_2Mg_{-1}Si_{-1}$ (tk), $KAlSi_{-1}$ (ed), and $NaSiAl_{-1}Ca_{-1}$ (pl). In samples from the study area, X_{tk} in amphibole ranges from 0.11 to 0.53, X_{ed} ranges from 0.08 to 0.24, and X_{pl} ranges from 0.00 to 0.06.

For dioctahedral and trioctahedral micas, the additive components are respectively end-member muscovite and phlogopite modified by simple cation exchanges plus the coupled substitutions tk, ed, and Al_2Fe_{-3} (dt). In dioctahedral micas, X_{tk} ranges from -0.07 to -0.15, X_{ed} ranges from 0.00 to -0.08, and X_{dt} ranges from 0.00 to -0.11. In trioctahedral micas, X_{tk} ranges from 0.20 to 0.39, X_{ed} ranges from -0.04 to -0.16, and X_{dt} ranges from 0.01 to 0.08. These data indicate that the coupled substitutions tk and ed are likely to have an important effect on the modal mineral assemblage, but the substitutions pl and dt are not.

Metamorphic reactions

Reaction set. Determining the controls on the distribution of metamorphic assemblages and the extent of fluid-rock interaction during metamorphism requires a thorough analysis of the reactions by which metamorphism proceeded. We have analyzed the reactions by which the Waits River Formation was metamorphosed using the reaction space technique of Thompson (1982b). The calcareous metasandstones of the Waits River Formation are described in a system of nine system components (C_s) and 30 phase components (C_p) (Table 2). This gives a total of 21 reactions, 14 of which are simple exchange reactions and seven of which are net transfer reactions. A set of linearly independent reactions that fully describes the net transfer reactions possible in this assemblage is given as Reactions 1–7 in Table 2.

TABLE 2. Net transfer reactions

Minerals	Additive components	Exchange components
Quartz	SiO_2 (QTZ)	
Calcite	$CaCO_3$ (CC)	fm, cm
Dolomite	$CaMg(CO_3)_2$ (DOL)	fm, cm
Muscovite	$KAl_3Si_3O_{10}(OH)_2$ (MUS)	fm, tk, ed, dt, nk
Biotite	$KMg_3AlSi_3O_{10}(OH)_2$ (BIOT)	fm, tk, ed, dt, nk
Tremolite	$Ca_2Mg_5Si_8O_{22}(OH)_2$ (TREM)	fm, cm, tk, ed, nk, pl
Plagioclase	$CaAl_2Si_2O_8$ (AN)	pl
Fluid	H_2O, CO_2	

System components: SiO_2 Al_2O_3 FeO MgO CaO Na_2O K_2O H_2O CO_2

Net transfer reactions:
(1) MUS + 3 DOL + 2 QTZ = BIOT + 2 CC + AN + 4 CO_2
(2) 5 DOL + 8 QTZ + H_2O = TREM + 3 CC + 7 CO_2
(3) AN + 2 CO_2 = TK + DOL + 3 QTZ
(4) AN + PL = ED + 4 QTZ
(5) 2 CC + AN + 4 CO_2 = DT + 3 DOL + 2 QTZ
(6) MUS + CC + NK + 2 QTZ = 2 AN + PL + H_2O + CO_2
(7) 2 CC = DOI + CM

Notes: Exchange component abbreviations as follows: tk = $Al_2Si_{-1}Mg_{-1}$; ed = $NaAlSi_{-1}$; dt = Al_2Mg_{-3}; pl = $NaSiCa_{-1}Al_{-1}$; cm = $CaMg_{-1}$; fm = $FeMg_{-1}$; nk = NaK_{-1}.

Reactions 1 and 2 describe the formation of pure biotite and tremolite, respectively. Reactions 3 and 4 describe the formation of exchange components tk and ed common to mica and amphibole. Reaction 5 describes the formation of the dioctahedral-trioctahedral exchange in micas. Reaction 6 is the breakdown of paragonite component in muscovite in the presence of calcite and quartz. Reaction 7 controls the composition of coexisting calcite and dolomite and is the two carbonate thermometer (Harker and Tuttle, 1955). All possible net transfer reactions in this system can be described as linear combinations of these seven reactions.

Tremolite and muscovite do not coexist in any of the samples studied suggesting that Reaction 2 proceeds only if muscovite is exhausted before dolomite in Reaction 1. Averaged whole rock major element analyses presented in Table 3 show that samples containing calcic amphibole have greater ferro-magnesian components relative to Al than samples containing muscovite. This probably reflects a greater abundance of dolomite relative to muscovite in the protoliths of these samples.

The dependence of mineral assemblages on bulk composition suggests that mineral-in isograds mapped using these assemblages may be misleading. However, as we

TABLE 3. Average whole-rock analyses

	Weight percent oxides			
Assemblage*	A	B	D	E
SiO_2	43.0	47.5	39.6	41.3
TiO_2	0.2	0.3	0.2	0.2
Al_2O_3	4.6	5.1	3.9	3.0
FeO	2.3	2.5	2.3	1.8
MnO	0.2	0.1	0.2	0.1
MgO	3.3	2.8	5.4	4.6
CaO	24.7	22.6	25.6	27.1
Na_2O	0.2	0.3	0.1	0.2
K_2O	1.1	1.2	0.8	0.8
P_2O_5	0.1	0.1	0.1	0.1
LOI**	20.3	17.6	21.5	20.9
Total	100.0	100.0	99.8	100.0
	Cation molar ratios			
(Al-Na)/FMMn†	1.14	1.29	0.71	0.65
3K/FMMn†	1.01	1.05	0.53	0.59
Number analyzed	3	2	1	4

* For explanation of assemblages see text.
** LOI = lost on ignition.
† FMMn = Fe + Mg + Mn.

TABLE 4. Modal abundances and calculated whole-rock reactions

	Modes (mol/L)					
	QTZ	CARB	PLAG	BIOT	MUSC	TREM
WR-73	10.943	15.298	0.467	0.687	0.249	—
WR-79	9.612	14.296	0.600	0.754	0.348	—
WR-82	18.707	11.101	0.182	0.220	0.554	—
WR-103	17.425	10.884	0.305	0.407	0.668	—
WR-56a	14.711	4.630	0.937	1.701	—	0.447
WR-83a	7.070	13.023	0.927	1.114	—	0.330
WR-83b	12.597	9.585	0.260	0.814	—	0.769
WR-100	12.761	13.538	0.633	0.800	—	0.073
WR-101	17.194	13.104	0.050	0.200	—	0.330
	Whole-rock reactions					
WR-73	0.508 QTZ + 0.030 H_2O + 1.448 DOL + 0.567 MUSC = 0.687 BIOT + 0.027 AB + 0.280 AN + 1.169 CC + 1.727 CO_2					
WR-79	0.674 QTZ + 0.021 H_2O + 1.687 DOL + 0.733 MUSC = 0.754 BIOT + 0.035 AB + 0.360 AN + 1.327 CC + 2.047 CO_2					
WR-82	0.168 QTZ + 0.003 H_2O + 0.491 DOL + 0.223 MUSC = 0.220 BIOT + 0.013 AB + 0.109 AN + 0.381 CC + 0.601 CO_2					
WR-103	0.321 QTZ + 0.014 H_2O + 0.890 DOL + 0.393 MUSC = 0.407 BIOT + 0.022 AB + 0.183 AN + 0.707 CC + 1.073 CO_2					
WR-56a	3.994 QTZ + 0.518 H_2O + 5.832 DOL + 1.630 MUSC + 0.024 AB = 1.701 BIOT + 0.447 TREM + 0.562 AN + 4.432 CC + 7.231 CO_2					
WR-83b	5.553 QTZ + 0.750 H_2O + 5.430 DOL + 0.833 MUSC + 0.070 AB = 0.814 BIOT + 0.769 + TREM + 0.156 AN + 3.815 CC + 7.045 CO_2					
WR-83a	3.212 QTZ + 280 H_2O + 4.087 DOL + 1.164 MUSC + 0.029 AB = 1.114 BIOT + 0.330 TREM + 0.556 AN + 2.894 CC + 5.281 CO_2					
WR-100*	1.205 QTZ + 0.091 H_2O + 2.160 DOL + 0.783 MUSC = 0.025 AB + 0.800 BIOT + 0.073 TREM + 0.380 AN + 1.640 CC + 2.680 CO_2					
WR-101*	2.250 QTZ + 0.323 H_2O + 1.983 DOL + 0.207 MUSC + 0.036 AB + 0.014 AN = 0.200 BIOT + 0.330 TREM + 1.376 CC + 2.589 CO_2					

Note: Reactions refer to net transfer in 1 L of rock. Ab = An + Pl exchange.
* Compositions of micas and amphibole assumed to be average of analyzed samples are muscovite: Si = 3.13, Al = 2.60, FMMn = 0.23, Na = 0.07, K = 0.92; biotite: Si = 2.84, Al = 1.48, FMMn = 2.50, Na = 0.90, K = 0.90; amphibole: Si = 7.48, Al = 0.91, FMMn = 4.65, Ca = 1.89, Na = 0.14, K = 0.03.

shall show in a later section, the dolomite-out isograd marks an important event in the metamorphic history of these rocks.

We suggest the following sequence for the appearance and disappearance of minerals during prograde metamorphism of the WRF: (1) formation of biotite, (2) disappearance of muscovite, (3) appearance of tremolite, and (4) disappearance of dolomite. This is the same sequence of prograde assemblages reported by Ferry (1987) and Hewitt (1973) for regionally metamorphosed calcareous sediments in New England.

Whole-rock reactions

Calculating the extent of fluid-rock interaction during metamorphism requires an estimation of the whole-rock reaction by which the original rock was transformed into the final metamorphic assemblage. In this study, we have calculated whole-rock reactions for metamorphosed calcareous sandstones by relating the observed assemblages to an idealized protolith consisting of assemblage O, quartz + albite + calcite + dolomite + muscovite. We have assumed that metamorphism is closed to all chemical species except CO_2 and H_2O.

Reaction progress along each of Reactions 1–7 can be quantified by (Thompson et al., 1982)

$$\xi_1 = \Delta n_{\text{biot}} = n_{\text{biot}}$$

$$\xi_2 = \Delta n_{\text{trem}} = n_{\text{trem}}$$

$$\xi_3 = \Delta n_{\text{tk}} = X_{\text{tk,biot}} n_{\text{biot}} + X_{\text{tk,amp}} n_{\text{trem}} + X_{\text{tk,musc}} n_{\text{musc}} - X_{\text{tk,musc}} n^0_{\text{musc}}$$

$$\xi_4 = \Delta n_{\text{ed}} = X_{\text{ed,biot}} n_{\text{biot}} + X_{\text{ed,amp}} n_{\text{trem}} + X_{\text{ed,musc}} n_{\text{musc}} - X_{\text{ed,musc}} n^0_{\text{musc}}$$

$$\xi_5 = \Delta n_{\text{dt}} = X_{\text{dt,biot}} n_{\text{biot}} + X_{\text{dt,musc}} n_{\text{musc}} - X_{\text{dt,musc}} n^0_{\text{musc}}$$

$$\xi_6 = \Delta n_{\text{nk}} = X_{\text{nk,biot}} n_{\text{biot}} + X_{\text{nk,amp}} n_{\text{trem}} + X_{\text{nk,musc}} n_{\text{musc}} - X_{\text{nk,musc}} n^0_{\text{musc}}$$

$$\xi_7 = \Delta n_{\text{cm}} = X_{\text{cm,amp}} n_{\text{trem}} \qquad (8)$$

where ξ_i is the extent of progress along Reaction i, $X_{j,k}$ is the mole fraction of exchange component j in mineral k (Thompson et al., 1982; Thompson, 1982a), n_k is the number of moles of mineral k in 1 L of sample, and n^0_k is the number of moles of mineral k in 1 L of the protolith.

Equations 8 determine the coordinates of the rock in net transfer reaction space (Thompson et al., 1982). The n_i's for additive components are determined by point counting and the X_i's are determined by microprobe analysis. The n_i^0's are evaluated by recalculating the compositions of amphibole and mica times the number of moles

TABLE 5. Metamorphic fluid composition

Sample	K_S	500 °C			525 °C			550 °C			Assemblage
		X_{H_2O}	X_{CO_2}	f_{O_2}	X_{H_2O}	X_{CO_2}	f_{O_2}	X_{H_2O}	X_{CO_2}	f_{O_2}	
WR-54d	0.273	0.950	0.049	−22.8	0.866	0.125	−22.2	0.678	0.318	−21.0	A
WR-54m	0.253	0.954	0.045	−22.9	0.892	0.107	−21.8	0.709	0.287	−21.0	A
WR-73	0.239	0.952	0.047	−22.8	0.888	0.110	−21.8	0.694	0.303	−21.0	A
WR-77	0.248	0.954	0.045	−22.9	0.888	0.110	−21.8	0.694	0.303	−21.0	A
WR-79	0.619	0.964	0.034	−23.0	0.922	0.076	−21.9	0.799	0.194	−21.0	A
WR-82	0.304	0.956	0.043	−22.9	0.899	0.099	−21.9	0.709	0.287	−21.0	A
WR-103	0.193	0.950	0.049	−22.8	0.866	0.125	−22.2	0.648	0.349	−20.9	A
WR-107	0.267	0.954	0.045	−22.9	0.895	0.103	−21.8	0.709	0.297	−21.0	A
WR-110	0.188	0.948	0.050	−22.8	0.866	0.125	−22.2	0.648	0.349	−20.9	A
WR-112	0.257	0.952	0.047	−22.8	0.892	0.107	−21.8	0.694	0.303	−21.0	A
WR-115	0.166	0.946	0.052	−22.8	0.859	0.133	−22.1	0.633	0.365	−20.9	A
WR-121	0.395	0.959	0.039	−22.9	0.911	0.087	−21.9	0.754	0.241	−21.0	A
WR-56a*	0.377	0.954	0.045		0.907	0.091		0.784	0.210		E
WR-83a*	0.904	0.959	0.039		0.922	0.076		0.821	0.171		E
WR-83b*	0.631	0.958	0.041		0.915	0.083		0.806	0.187		E
WR-85a*	0.585	0.957	0.042		0.915	0.083		0.806	0.187		E
WR-85d*	0.889	0.959	0.039		0.922	0.076		0.821	0.171		E
WR-87*	0.714	0.958	0.041		0.919	0.079		0.814	0.179		E
WR-200*	0.925	0.959	0.039		0.922	0.076		0.828	0.163		E

* X_{Mg} in dolomite assumed to equal 0.8.

of each present in terms of the minerals in the protolith plus H_2O and CO_2 (Thompson et al., 1982). For samples that contain no muscovite, the composition of the muscovite in the protolith is assumed to be the average of muscovites from the study area. After determining ξ for each of Reactions 1–7, the whole-rock reaction can be determined by summing the net effect of each reaction on the assemblage.

Representative modal data and calculated whole rock reactions are given in Table 4 in terms of moles/liter of rock. In samples for which we have modal data but no compositional data, the compositions of micas and amphibole are assumed to be the average of samples analyzed from the study area, given in Table 4. If our assumptions about the protolith from which these samples formed are correct, then prograde metamorphism of the WRF evolved considerable CO_2. Additionally, the formation of calcic amphibole consumed considerable H_2O. Infiltration of H_2O for the formation of amphibole is required if the assumed protolith assemblage is correct. Minor chlorite (<3% of mode) is the only other hydrous phase in these rocks and is not believed to be responsible for the formation of calcic amphibole in these samples.

Fluid buffering and composition during metamorphism

The dolomite-out isograd marks an important event with regards to fluid composition during prograde metamorphism of the WRF. In assemblages A and D, the fluid composition is buffered by the isobaric univariant equilibria defined by Reactions 1 and 2, respectively (Rice and Ferry, 1982). Assemblages B, C, and E, however, do not confine the fluid composition to univariant equilibria. Thus, the dolomite-out isograd, which separates assemblages A and D from assemblages B, C, and E, represents the point at which the rocks lose their capacity to buffer the fluid composition to a univariant curve during metamorphism.

In assemblage A, Reaction 1 defines the value of X_{CO_2} of the fluid phase at a given P and T (Ferry and Burt, 1982, Eq. 46). Because assemblage A includes graphite, the composition of the fluid can be further constrained to lie on the graphite saturation boundary in the system C-O-H (Ohmoto and Kerrick, 1977). The composition of the ternary C-O-H fluid in equilibrium with assemblage A can be calculated by simultaneous solution of Ferry and Burt's Equation 46 and Ohmoto and Kerrick's Equations 2–5 and 11. Additionally, the equations of Ohmoto and Kerrick (1977) provide a calculation of f_{O_2} during metamorphism.

Metamorphic fluid compositions were calculated at 500, 525, and 550 °C at 6.0 kbar (Table 5). Fugacity coefficients of CO_2, H_2O, and CH_4, and expressions for nonideal mixing of fluid species are from Jacobs and Kerrick (1981) and Kerrick and Jacobs (1981). Fugacity coefficients of H_2 and CO are from Ryzhenko and Volkov (1971). Mineral activity models used are the same as in Ferry (1987) except for the use of the activity coefficient of Newton and Haselton (1981) for feldspar. Equilibrium cooeficients for mineral phases (K_s) used to calculate fluid compositions are given in Table 5. Values of K_d for equations describing the devolatilization of graphite are from Ohmoto and Kerrick (1977). The enthalpy, entropy, and volume change of reaction are from Ferry (1987).

Calculated fluid compositions are essentially binary CO_2-H_2O fluids (Table 5) because of the position of the graphite saturation boundary at these pressure-temperature conditions (cf. Rumble and Hoering, 1986; Duke and Rumble, 1986). At 500 °C, X_{H_2O} for samples with assemblage A varies from 0.97 to 0.94 and at 550 °C X_{H_2O} varies from 0.85 to 0.53. Calculated values of fluid composition and f_{O_2} are stongly dependent on the estimated temperature and to a lesser extent on the composition of the minerals present.

Fluid compositions for samples containing assemblage

TABLE 6. Time integrated fluid/rock ratios

Sample	Assemblage	N_{int} 500 °C	N_{int} 525 °C	N_{int} 550 °C	f/r 500 °C	f/r 525 °C	f/r 550 °C	f/r isotopic
				Orange anticline				
WR-73	A	35.0	14.0	—	0.424	0.169	—	0.258
WR-77	A	44.3	16.9	—	0.537	0.205	—	0.300
WR-79	A	58.2	24.9	—	0.726	0.311	—	—
WR-75*	A	38.5	15.0	—	0.467	0.182	—	0.401
WR-71a**	D	88.4	43.0	—	1.071	0.521	—	0.898
				Grannyhand anticline				
WR-56a	E	154.0	72.7	—	1.880	0.888	—	0.811
				Old City syncline				
WR-100**	E	—	30.5	12.2	—	0.369	0.148	0.413
WR-101**	E	—	29.7	12.0	—	0.354	0.144	0.606
WR-103	A	—	7.5	2.0	—	0.091	0.024	0.063
WR-107	A	—	19.8	5.4	—	0.244	0.067	0.088
WR-115	A	—	20.4	5.5	—	0.247	0.066	0.171
WR-121	A	—	28.6	8.6	—	0.348	0.105	0.281
WR-151a*	B	—	16.7	4.8	—	0.201	0.057	0.195
WR-151b*	B	—	31.6	9.0	—	0.386	0.110	0.294
WR-151c*	B	—	30.1	8.6	—	0.366	0.104	0.405
WR-151d*	B	—	15.8	4.5	—	0.190	0.054	0.332
WR-151h*	B	—	1.4	0.4	—	0.016	0.005	0.259
WR-151j*	B	—	6.1	1.7	—	0.074	0.021	0.422
				Strafford syncline				
WR-49**	E	—	34.1	13.7	—	0.419	0.169	0.339
WR-82	A	—	5.5	1.5	—	0.067	0.018	0.171
WR-83a	E	—	64.5	25.9	—	0.787	0.316	0.403
WR-83b	E	—	78.6	31.4	—	0.932	0.372	0.042
WR-85a	E	—	59.3	23.7	—	0.702	0.280	0.232
WR-85c**	E	—	57.7	23.4	—	0.695	0.281	0.158
WR-85d	E	—	70.6	28.5	—	0.852	0.344	0.132
WR-85e	E	—	66.9	27.2	—	0.797	0.324	0.121
WR-85f**	E	—	68.1	27.6	—	0.814	0.330	0.127
WR-87	E	—	36.0	14.3	—	0.437	0.174	0.067
WR-110	A	—	12.3	3.3	—	0.150	0.040	0.009
WR-112	A	—	2.7	0.8	—	0.033	0.009	0.081
WR-201*	E	—	74.1	29.9	—	0.903	0.364	—

* X_{CO_2} = average from assemblage A.
** X_{CO_2} = average from assemblage E.

E were estimated using the equilibrium defined by Reaction 2 (Table 2). Dolomite is absent in assemblage E, so application of the equilibrium defined by Reaction 2 requires that a composition for dolomite be assumed ($X_{Mg,dol}$ = 0.8). The absence of dolomite constrains the metamorphic fluid composition to lie to the H_2O rich side of the univariant curve defined by the equilibrium and as such yields a minimum value of X_{H_2O} in the fluid (cf.

TABLE 7. Stable isotopic data

Sample	$\delta^{13}C$ (‰)	$\delta^{18}O$ (‰)	Sample	$\delta^{13}C$ (‰)	$\delta^{18}O$ (‰)	Sample	$\delta^{13}C$ (‰)	$\delta^{18}O$ (‰)	Sample	$\delta^{13}C$ (‰)	$\delta^{18}O$ (‰)
WR-41	−3.3	12.0	WR-55b	−1.3	16.8	WR-85b	−1.0	18.8	WR-112	−1.3	19.5
WR-42	−2.2	18.3	WR-56a	−2.6	15.6	WR-85c	−1.1	18.9	WR-113	−3.5	18.1
WR-43	−2.7	15.4	WR-57	−1.6	16.7	WR-85d	−1.0	19.0	WR-114	−1.1	18.8
WR-44	−2.0	16.7	WR-58	−0.8	17.7	WR-85e	−1.2	18.9	WR-115	−0.3	18.8
WR-49	−1.0	17.7	WR-70c	−2.1	15.9	WR-85f	−1.1	18.7	WR-116	0.1	20.6
WR-49	−1.2	17.7	WR-71a	−1.9	15.7	WR-86	−2.2	18.9	WR-118	−0.7	19.6
WR-50	0.8	19.2	WR-71b	−2.4	16.1	WR-87	−1.4	19.4	WR-119	−2.0	17.4
WR-51	−1.1	18.2	WR-72	−2.2	18.3	WR-89	−1.4	19.4	WR-120	−2.0	18.1
WR-52	−2.0	18.8	WR-73	−0.8	18.4	WR-90	−2.3	18.3	WR-121	−1.2	18.2
WR-54	−1.7	19.3	WR-75	−0.5	17.9	WR-100	−2.8	17.5	WR-122	−1.3	17.0
WR-54b	−2.4	18.5	WR-76	−0.8	17.4	WR-101	−2.3	16.6	WR-123	−0.5	16.1
WR-54c	−2.7	17.3	WR-77	−0.1	18.4	WR-102	−0.1	20.1	WR-125	−2.3	18.8
WR-54d	−2.4	17.7	WR-78	−0.9	18.2	WR-103	−1.5	19.5	WR-126	−1.5	19.1
WR-54e	−3.1	17.3	WR-79	−0.4	21.0	WR-104	−1.0	20.2	WR-127	−1.6	20.5
WR-54i	−2.7	17.5	WR-81	−3.3	17.4	WR-106	−0.7	20.5	WR-128	−1.5	18.4
WR-54ii	−2.6	17.6	WR-82	−1.1	18.8	WR-107	−0.9	19.3	WR-129	−1.3	17.5
WR-54iii	−2.7	17.6	WR-83A	−1.2	17.5	WR-108	−1.1	18.6	WR-151a	−1.1	18.4
WR-54j	−2.4	18.3	WR-83B	−1.0	19.4	WR-109	−1.5	20.6	WR-151b	−1.0	18.6
WR-54m	−2.5	18.1	WR-84	−1.9	17.3	WR-110	−1.4	19.9	WR-151c	−1.2	18.0
WR-54o	−2.0	19.7	WR-85a	−1.5	18.3	WR-111	−1.5	17.8	WR-151d	−1.0	17.8

Ferry, 1987). Estimated values of X_{H_2O} in samples containing assemblage E are higher at a given temperature than those calculated for assemblage B (Table 5). As for assemblage A, X_{H_2O} calculated for assemblage E is also highly dependent on temperature.

Time integrated fluid/rock ratios

The composition of the fluids generated by prograde metamorphism of the WRF (Table 4) is different from our calculated equilibrium fluid compositions (Table 5). Such a difference has been cited as evidence for fluid infiltration during metamorphism (Ferry, 1987; Tracey et al., 1983; Rumble et al., 1982; Hoisch, 1987). Given the equilibrium fluid composition and prograde reaction history, the minimum amount of fluid infiltration required to maintain an equilibrium fluid composition during prograde metamorphism can be calculated (Ferry, 1986).

We have applied Ferry's (1987) Equation 5 to the results summarized in Tables 4 and 5 for temperatures of 500, 525, and 550 °C (Table 6). Results are expressed both as moles of H_2O infiltrated (N_{inf}) and as time integrated fluid/rock ratios (f/r) in O equivalents. For samples for which mineral composition data were not known, an average value of X_{CO_2} was used. These f/r represent minimum estimated values because (1) the composition of the infiltrating fluid is assumed to be pure H_2O, and (2) samples cease to record fluid infiltration petrologically when reactant minerals are exhausted by reaction progress (Ferry, 1987).

Within individual fold hinge zones, samples from within the dolomite-out isograd record higher f/r than those from outside the isograd (Table 6). This is due to the greater reaction progress that these samples record. According to the model of fluid infiltration–driven metamorphism (Ferry, 1987), samples from inside the dolomite-out isograd were subjected to greater infiltration of hydrous fluids during metamorphism than those from outside the isograd.

If the model of metamorphism driven by fluid infiltration is appropriate for the WRF, then the distribution of dolomite-absent assemblages in the SS, OCS, and GA suggests that hydrous fluids flowed into the WRF from the direction of the SPV and CGS. Had fluid flow been in the opposite direction, then the rocks surrounding the dolomite-out isograd would have recorded this flow through greater reaction progress.

If the model of metamorphism driven by fluid infiltration is not appropriate for the WRF, then the dolomite-out isograd must be related to something other than fluid infiltration and must be further considered. In order to test whether the WRF was infiltrated by hydrous fluids, we examined the stable isotopic systematics of the WRF, SPV, and CGS.

Stable isotopic study

The isotopic compositions of C and O in carbonate were measured in 91 samples of calcareous metasandstones from the Waits River Formation. The O isotopic composition of quartz was measured for 11 samples of calcareous metasandstones and eight samples of interbedded pelites and veins in the Waits River Formation, eight samples of coarse garnet schist, and 13 samples of Standing Pond Volcanics. C and O isotopic compositions are reported in δ notation relative to PDB and SMOW, respectively (Table 7). Multiple samples from the same outcrop are denoted by lower case letter suffixes.

Values of $\delta^{13}C_{carb}$ range from +0.8‰ to −3.5‰. Values of $\delta^{18}O_{carb}$ range from 21.0‰ to 15.6‰ in samples stratigraphically below the SPV and from 17.7‰ to 15.4‰ in samples stratigraphically above the SPV. One sample has a $\delta^{18}O_{carb}$ value of 12.0‰. O isotope analyses of quartz from eight samples of coarse garnet schist average 16.4‰

Table 7—*Continued*

Sample	$\delta^{13}C$ (‰)	$\delta^{18}O$ (‰)	Quartz from WRF			Quartz from CGS		Quartz from SPV	
			Sample	Sample type	$\delta^{18}O$ (‰)	Sample	$\delta^{18}O$ (‰)	Sample	$\delta^{18}O$ (‰)
WR-151e	−1.0	18.0	WR-54d	carb.	19.0	WR-56b	16.7	SP101	11.6
WR-151f	−1.0	18.1	WR-54f	pelite	19.1	SP102	16.4	SP104	14.2
WR-151g	−1.0	17.9	WR-54i	carb.	18.9	SP131	15.6	SP105	13.9
WR-151h	−0.6	17.7	WR-54h	pelite	18.8	SP137	17.3	SP106	14.0
WR-151j	−0.7	17.2	WR-54m	carb.	19.4	SP200	17.2	SP106 vein	12.3
WR-152	−1.7	16.9	WR-54n	pelite	19.3	SP201	17.1	SP108	11.8
WR-153	0.1	19.4	WR-54	vein	19.3	SP204	15.1	SP131	13.2
WR-154	−1.4	17.5	WR-44	carb.	18.5	SP206	16.0	SP132	12.5
WR-207b	−1.1	18.0	WR-44	pelite	18.7			SP133	13.8
WR-208	−1.4	19.4	WR-44	vein	18.0			SP135	12.9
WR-209	−1.6	18.5	WR-100	carb.	19.3			SP138	13.9
			WR-100	pelite	20.3			SP203	12.4
			WR-100	vein	19.6			SP205	13.8
			WR-85b	carb.	20.7			SP207	12.8
			WR-85b	vein	20.1			SP209	12.3
			WR-85c	carb.	20.8				
			WR-85d	carb.	20.8				
			WR-85e	carb.	20.7				
			WR-85f	carb.	20.6				
			WR-85g	carb.	20.3				

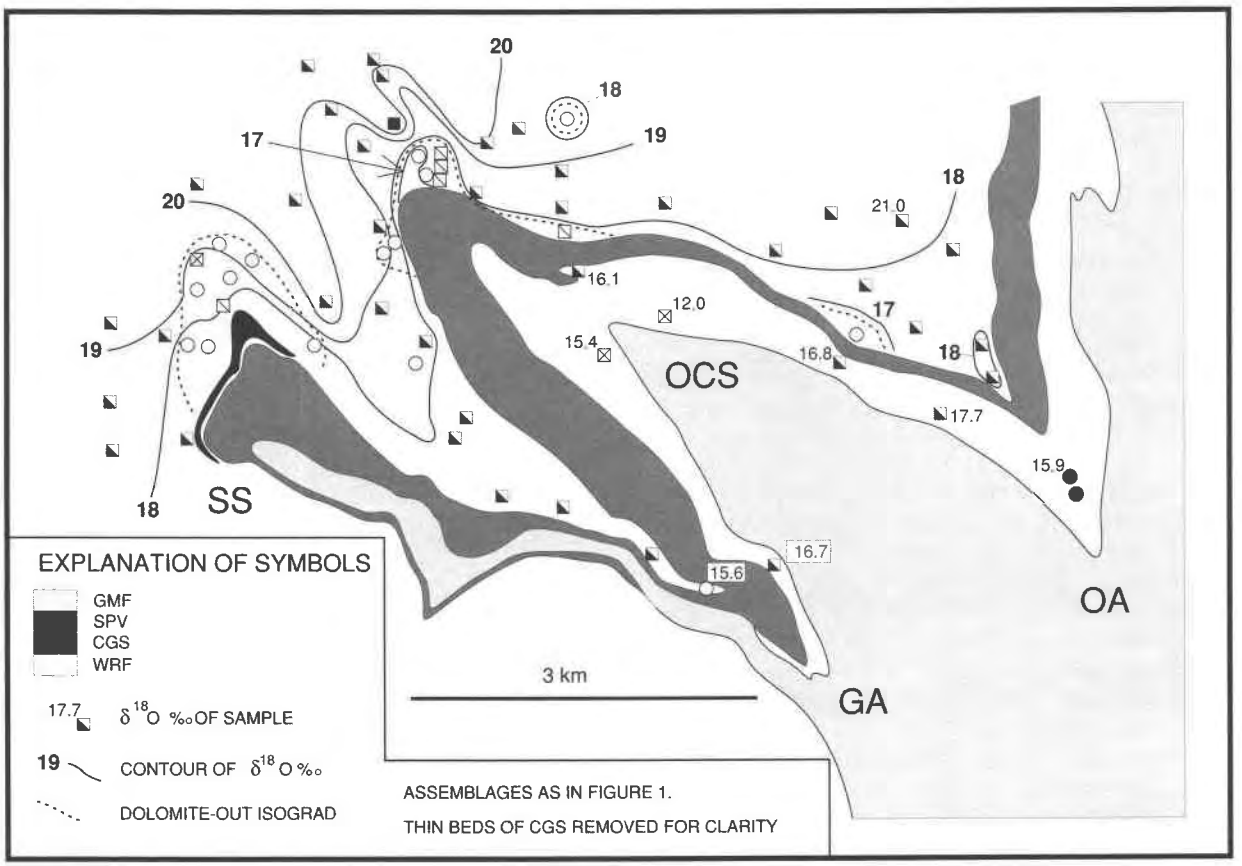

Fig. 3. Map of the study area with contours of $\delta^{18}O$ in carbonate. Thin beds of coarse garnet schist removed for clarity.

and 14 samples of Standing Pond Volcanics average 13.1‰.

Values of $\delta^{18}O_{carb}$ in the Waits River Formation are contoured on the map in Figure 3. Contours of $\delta^{18}O_{carb}$ are roughly parallel to the contact between the Waits River Formation and Standing Pond Volcanics with less enriched values nearer the Standing Pond Volcanics. In the Old City syncline, the dolomite-out isograd is coincident with the $\delta^{18}O_{carb}$ = 18‰ contour. In the Strafford syncline however, the dolomite-out isograd crosses both the $\delta^{18}O_{carb}$ = 18‰ and 19‰ contours.

The contours of $\delta^{18}O_{carb}$ broadly mimic the fold pattern in the Strafford area (Fig. 3). It is possible that the isotopic composition of the carbonates are primarily a function of stratigraphic position and simply reflect the bulk composition of the rock. If this were the case, then there would be little evidence for interaction with an isotopically reactive fluid on a regional scale. Several pieces of evidence suggest that the variations in $\delta^{18}O_{carb}$ are not simply the result of stratigraphic variation.

1. Within the study area, the WRF is lithologically uniform throughout. There is no regular variation in bedding type, thickness, or composition with stratigraphic position.

2. In some terranes, enrichment of ^{18}O correlates positively with the modal abundance of carbonate (Sheppard and Schwarcz, 1970; Valley and O'Neil, 1984). Figure 4 does not show this correlation for samples from the WRF, so it is unlikely that variations in modal abundance of carbonate are responsible for the observed isotopic variations.

3. In outcrop 85, sample WR-85b contains muscovite while all other samples contain tremolite. The different modal assemblages result from variations in bulk composition (Table 3), yet all quartz samples analyzed from outcrop 85 are isotopically homogeneous within analytical uncertainty.

4. In outcrop 54, quartz samples from both calcareous metasandstones and interbedded pelites are isotopically homogeneous within analytical uncertainty, again suggesting that bulk composition does not affect isotopic ratios within the WRF.

It is also possible that the pattern of isotope depletion shown in Figure 3 was formed by fluid-rock interaction prior to deformation and was subsequently folded with the strata. It is not possible to differentiate between fluid-rock interactions that were prefolding and postfolding from the isotopic data alone. However, petrographic examination shows that calcic amphibole crystals cut across the axial planar foliation defined by micaceous minerals,

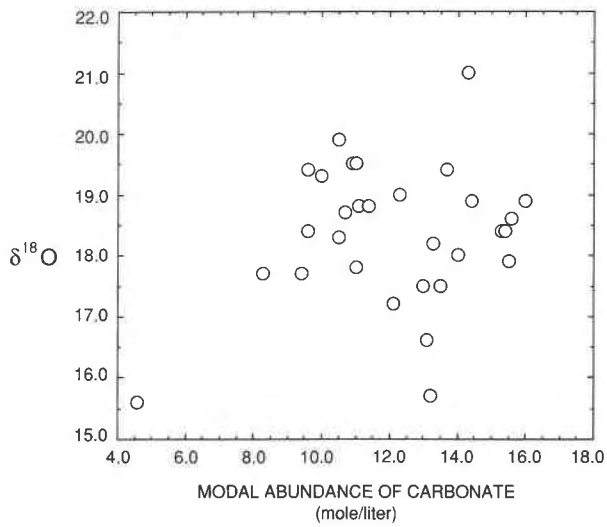

Fig. 4. Scatter plot of $\delta^{18}O$ in carbonate vs. modal abundance of carbonate.

Table 8. Isotopic fractionation factors

				References
C				
CO_2-CC	$-2.4612 + 7.6663E3/T - 2.9880E6/T^2$			1
O				
$1000 \ln(a) = A*10^6/T^2 + B*10^4/T + C$				
	A	*B*	*C*	
CC-QTZ	−0.38	—	—	2
CC-DOL	−0.50	—	—	3
CC-AB	0.57	—	—	2
CC-AN	1.59	—	—	2
QTZ-MUSC	2.20	—	−0.60	4
QTZ-AMP	1.554	—	−0.30	4
QTZ-BIOT	3.690	—	−0.60	4
QTZ-H_2O	2.05	—	−1.14	5
CC-CO_2	1.8034	−1.0611	3.2798	1

Note: References: 1 = Bottinga, 1968; 2 = Clayton et al., 1989; 3 = Northrup and Clayton, 1966; 4 = Bottinga and Javoy, 1975; 5 = Matshisa et al., 1979.

suggesting that they grew after the isoclinal folding event that formed the foliation. Because our petrologic studies indicate that calcic amphibole grew as a result of fluid infiltration, we suggest that the O isotopic systematics of the WRF are the result of fluid infiltration that occurred during and after the isoclinal folding event.

Modeling of the isotopic data

A number of quantitative models have been proposed to describe shifts in isotopic composition as a result of fluid infiltration (Taylor, 1973, 1978; Nabelek, 1987; Baumgartner and Rumble; 1988). Before observed variations in isotopic composition can be attributed to fluid infiltration, however, the effect of net transfer reactions on the isotopic compositions must first be quantified (Broecker and Oversby, 1971; Rumble et al., 1982; Valley, 1986; Chamberlain et al., 1990).

C isotopes. The effect of Rayleigh distillation on the C isotopic composition of carbonates during metamorphism of the Waits River Formation was calculated by (Broecker and Oversby, 1971)

$$\delta^{13}C_{carb}^{final} - \delta^{13}C_{carb}^{init} = 1000(F^{\alpha-1} - 1) \quad (9)$$

where $\delta^{13}C_{carb}^{final} - \delta^{13}C_{carb}^{init}$ is the change in $\delta^{13}C_{carb}$, α is the isotopic fractionation factor, and F is the fraction of unreacted carbonate given by

$$F = N_{carb}^{obs}/(N_{carb}^{obs} + N_{Co_2}^{rxn}) \quad (10)$$

where N_{carb}^{obs} is the number of moles of carbonate per unit volume of rock and $N_{CO_2}^{rxn}$ is the number of moles of CO_2 evolved during prograde metamorphism per unit volume of rock. Isotopic fractionation factors (α) used in our isotopic models are given in Table 8.

Table 9 and Figure 5 summarize the results of calculated shifts in $\delta^{13}C$ caused by Rayleigh distillation. Samples with original values of $\delta^{13}C = 0‰$ that were subse-

Table 9. Calculated and observed isotopic shifts

		Shift in $\delta^{13}C$		Shift in $\delta^{18}O$	
Sample	1-F*	Calculated**	Observed†	Calculated‡	Observed§
		Orange anticline			
WR-71a	0.222	−0.6	−1.9	−0.07	−4.3
WR-73	0.109	−0.3	−0.8	0.03	−1.6
WR-75	0.103	−0.3	−0.6	0.07	−2.2
WR-77	0.121	−0.3	−0.2	0.08	−1.6
WR-79	0.125	−0.3	−0.4	0.01	1.0
		Grannyhand anticline			
WR-56a	0.610	−2.4	−2.6	−0.41	−4.4
		Old City syncline			
WR-100	0.165	−0.5	−2.8	−0.04	−2.6
WR-101	0.165	−0.5	−2.3	−0.13	−3.4
WR-103	0.093	−0.2	−1.5	−0.03	−0.5
WR-107	0.186	−0.5	−0.9	−0.05	−0.7
WR-110	0.142	−0.4	−1.4	−0.05	−0.1
WR-112	0.029	−0.1	−1.3	0.16	−0.5
WR-115	0.211	−0.6	−0.3	−0.05	−1.2
WR-121	0.170	−0.5	−1.2	−0.02	−1.8
WR-151a	0.169	−0.5	−1.1	−0.12	−1.6
WR-151b	0.190	−0.5	−1.0	0.10	−1.4
WR-151c	0.199	−0.6	−1.2	0.06	−2.0
WR-151d	0.145	−0.4	−1.0	−0.07	−2.2
WR-151h	0.017	−0.0	−0.6	−0.34	−2.3
WR-151j	0.057	−0.1	−0.7	−0.07	−2.8
		Strafford syncline			
WR-49	0.265	−0.8	−1.1	−0.19	−2.3
WR-82	0.052	−0.1	−1.1	−0.02	−1.2
WR-83a	0.289	−0.9	−1.2	−0.13	−2.5
WR-83b	0.424	−1.4	−1.0	−0.32	−0.6
WR-85a	0.337	−1.0	−1.5	−0.25	−1.7
WR-85c	0.259	−0.7	−1.1	−0.18	−1.1
WR-85d	0.319	−1.0	−1.0	−0.23	−1.0
WR-85e	0.267	−0.8	−1.2		
WR-85f	0.357	−1.1	−1.1	−0.27	−1.3
WR-87	0.177	−0.5	−1.3	−0.12	−0.6

* Value of *F* from Equation 10 in text.
** Shift based on Rayleigh distillation, Equation 9 in text.
† Observed shift in $\delta^{13}C$ based on protolith value of 0.0‰.
‡ Calculated shift based on lever rule effects plus Rayleigh distillation (see text for explanation).
§ Observed shift in $\delta^{18}O$ based on protolith value of 20.0‰.

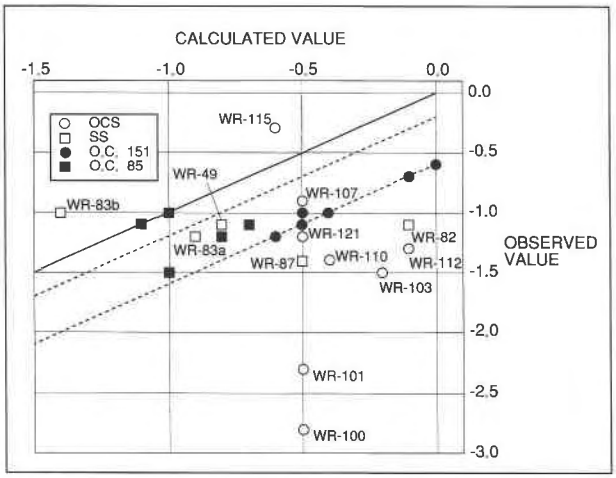

Fig. 5. Calculated shifts in $\delta^{13}C$ vs. observed values of $\delta^{13}C$ in carbonates from the Old City and Strafford synclines. Samples with protolith values of $\delta^{13}C = 0$ that were altered by Rayleigh fractionation would plot on the solid line through the origin. Samples from outcrops 151 and 85 lie on or near lines parallel to this line but displaced from it, suggesting C isotopic heterogeneities in the protoliths subsequently altered by Rayleigh fractionation.

quently altered by Rayleigh distillation as a result of reaction progress would plot on the diagonal line through the origin. Samples with a different original value of $\delta^{13}C$ that have been affected by Rayleigh distillation would plot on a line parallel to but displaced from the solid line.

Five of six samples from outcrop 151 fall on a line indicating an original $\delta^{13}C$ value of -0.6‰. Samples from outcrop 85 fall near a less well defined line indicating an original $\delta^{13}C$ value of approximately -0.2‰. We take the data from outcrops 151 and 85 as evidence that (1) Rayleigh distillation had an important effect on the C isotopic composition of these rocks, and (2) there was some heterogeneity in the C isotopic composition of the protoliths.

Some samples, e.g., WR-100 and WR-101 have values of $\delta^{13}C$ much depleted relative to other samples. This may be caused by (1) infiltration of isotopically light C into these samples; (2) large variations in the C isotopic composition of carbonate in the protoliths; or (3) varying amounts of organic C in the protoliths (cf. Valley, 1986). Given the fine grained nature of the graphite in these samples and the difficulty in assessing the C isotopic composition of the protoliths, evaluating these possibilities is difficult at best and will not be considered further in this paper.

Lever rule effects on O isotopes. The equation of Broecker and Oversby is inadequate to calculate shifts in $\delta^{18}O_{carb}$ resulting from reaction progress because O is distributed among multiple phases. We have used Rumble's (1982) numerical model of combined Rayleigh distillation and lever rule effects in order to model observed variations in $\delta^{18}O_{carb}$. We have assumed a rock porosity of 0.1%, isothermal reaction progress at 525 °C, and the isotopic fractionation factors in Table 8. Varying the assumed porosity over 3 orders of magnitude has no detectable effect on the calculated shift in isotopic composition, and varying the assumed temperature over the range of estimated temperatures of metamorphism within the study area has an effect of less than ±0.1‰. The choice of isotopic fractionation factors has a similarly small effect on these calculations.

Combined distillation and lever rule effects calculated for these samples amount to shifts in $\delta^{18}O_{carb}$ of between -0.4 and $+0.1$‰ and are for the most part between 0.0 and -0.2‰ (Table 9). Comparison of relatively unreacted dolomite-bearing samples with more reacted dolomite-absent samples shows that these rocks actually experience a negative shift in $\delta^{18}O_{carb}$ of up to -4‰ during metamorphism. In order to account for the relatively large negative $\Delta^{18}O^{rxn}$, the Waits River Formation must have been infiltrated by O-bearing fluids depleted in ^{18}O during metamorphism.

Infiltration effects on O isotopes. We have calculated fluid/rock ratios using the equations of Rumble (1982) in order to determine the minimum amount of fluid infiltration required to generate the pattern of ^{18}O depletion in carbonates in the WRF. We have used the same assumptions as before plus an initial $\delta^{18}O_{carb}$ of 20.0‰ and an infiltrating fluid of pure H_2O in isotopic equilibrium with quartz from the SPV ($\delta^{18}O_{H_2O} = 11.0$‰). Like the *f/r* determined from petrologic considerations, these ratios are expressed as moles of O in the infiltrating fluid to moles of O in the observed assemblage. Also like the petrologic *f/r*, these represent minimum estimates because they assume that the infiltrating fluid undergoes no isotopic exchange before it reaches the sample.

Isotopic *f/r* range from 0.01 to 0.90 (Table 6). For samples from the OA, *f/r* determined by petrologic methods fall in the range of *f/r* determined by petrologic methods for all samples except WR-79, for which $\delta^{18}O_{carb} = 21.0$‰. The O isotopic composition of this sample cannot be modeled by this method assuming a protolith value of 20‰.

Several samples from inside the dolomite-out isograd in the OCS record isotopic *f/r* greater than petrologic *f/r*. This is not surprising because rocks will cease to record fluid infiltration petrologically when the dolomite-out isograd is exceeded. Also, it is likely that the infiltrating fluid is not pure H_2O, so that the actual amount of fluid infiltration will be greater than the minimum calculated petrologically. Petrologic and isotopic *f/r* are in agreement for samples from outside the dolomite-out isograd in the OCS.

All but one of the samples from inside the dolomite-out isograd in the SS record higher petrologic than isotopic *f/r*. We suggest that these samples have either (1) been metamorphosed at a higher temperature than 550 °C or (2) interacted with fluids isotopically different from the fluids with which other samples interacted. The first situation is suggested by the fact that one sample from the CGS in the SS records a garnet-biotite temperature

of 583 °C (Barnett and Chamberlain, in preparation). Increased temperature reduces the petrologic *f/r*. The possibility that there was interaction with an isotopically different fluid is suggested by the proximity of the particularly thick layer of CGS which lies between the SPV and WRF in this syncline. An infiltrating fluid in isotopic equilibrium with the CGS rather than the SPV would be less depleted in ^{18}O by about 3‰, thus increasing the isotopic *f/r*. We are unable to resolve which of these two possibilities is most likely given the data.

Discussion

Thermal heterogeneities and metamorphism

Dolomite-absent assemblages occur over wide areas in synclinal fold hinges and over more restricted areas away from synclinal fold hinges. This pattern indicates that reaction progress is enhanced in synclinal fold hinges relative to anticlinal fold hinges. The difference in the amount of reaction progress between synclinal and anticlinal hinge zones could be caused by either increased temperature or increased fluid infiltration in synclinal fold hinges during metamorphism. The pattern of ^{18}O depletion in samples from the Waits River Formation, however, does not indicate increased infiltration in synclinal fold hinges relative to anticlinal fold hinges. Equally depleted $\delta^{18}O$ values occur in both anticlines and synclines suggesting that the amount of infiltration was about equal in both.

If anticlines and synclines were subjected to the same amount of fluid infiltration, our calculations show that the difference in reaction progress between anticlines and synclines can be accounted for by a temperature difference of less than 50 °C during metamorphism (Tables 5, 6). Geothermometry studies conducted on samples from pelitic schists indicate that synclinal fold hinges reached temperatures 20 to 60 °C higher than anticlinal fold hinges during metamorphism (Barnett and Chamberlain, in preparation). We therefore conclude that the enhanced reaction progress in synclines relative to anticlines displayed by the Waits River Formation is the result of the higher temperature of metamorphism reached in synclinal folds. This result is consistent with the studies of Sleep (1979), Fisher (1980), and Chamberlain (1986) who showed that synclinal folds can be expected to experience increased temperatures relative to anticlinal folds if deformation rates are sufficiently rapid.

Fluid infiltration and metamorphism

Within individual synclinal fold hinges, the dolomite-out isograd separates samples that record greater reaction progress from samples that record less reaction progress. Large differences in the extent of reaction occur over length scales of only hundreds of meters (compare sample WR-101 with WR-102, and WR-83a and WR-83b with WR-82, Table 4, Fig. 1). Since thermal heterogeneities over such short length scales are erased over very short time scales (Sleep, 1979), the difference in reaction progress between samples within the same fold hinge must be caused by a difference in the amount of fluid infiltration. O isotopic data support greater fluid infiltration within the dolomite-out isograd in the hinge zones of the OCS and GA, where samples from inside the isograd are much depleted compared to samples from outside the isograd. This relationship is less clear in the SS where contours of $\delta^{18}O$ cross the dolomite-out isograd. Despite equivocal isotopic data within the SS, we conclude that differences in the amount of reaction progress recorded by samples from within a given fold hinge resulted from differences in the amount of hydrous fluid locally available to drive hydration-decarbonation reactions.

Fluid sources

Petrologic considerations show that infiltration of hydrous fluids is required for fluid-present metamorphism in the WRF. Stable isotopic considerations suggest that ^{18}O-depleted fluids were transferred from the SPV and CGS to the WRF. The purpose of the following discussion is to determine whether dehydration reactions in the SPV and CGS could have provided the amount of fluid necessary for fluid present metamorphism, or whether an external source of fluid must have been involved.

The SPV in the amphibolite facies of metamorphism typically contain about 50% modal hornblende (Boxwell, 1986). Thompson et al. (1982) showed that the SPV and other amphibolites in east Vermont were formed largely be the reaction 12 epidote + 7 chlorite + 14 quartz = 12 tremolite + 25 tk + 22 H_2O (Thompson et al., 1982, Reaction 12). The number of moles of H_2O released by the above dehydration reaction ($N^{H_2O}_{rxn}$) in an amphibolite that contains 50% hornblende is about 3.5 mol/L.

The CGS is too coarse grained to be point counted in thin section, but we estimate that the unit contains about 20% modal garnet. A schist that forms garnet by the reaction muscovite + 3 chlorite + 3 quartz = biotite + 4 garnet + 12 H_2O will release 0.26 mol of H_2O per modal percent almandine garnet. A schist that contains an average of 20% modal garnet may be expected to release about 5.2 mol/L of H_2O during prograde metamorphism.

The average amount of fluid infiltration calculated for samples from inside the dolomite-out isograde in the WRF at 550 °C is 17.2 mol of H_2O/L of rock (Table 6). The WRF consists of about one half calc-silicate beds and one half micaceous quartzites. Because the quartzites neither produce CO_2 nor consume H_2O during metamorphism, it follows that a column of average WRF inside the dolomite-out isograd requires a column of SPV that is about 2.5 times as thick to provide sufficient H_2O for the amount of reaction progress observed. The same column of WRF requires a column of CGS that is about 1.7 times as thick.

In the Old City syncline, the thickness of the SPV relative to the dolomite-absent zone in the WRF is approximately 2.5 to 1. Dehydration of the SPV by the above reaction represents a sufficient source of hydrous fluid to account for reaction progress in the WRF in the Old City syncline. In the hinge zone of the Strafford syncline, the relative thicknesses of the SPV, CGS, and the dolomite-

absent zone in the WRF is about 1 to 0.5 to 1 (Fig. 1). If the SPV and the CGS were metamorphosed by the reactions suggested above, then fluids derived from dehydration of these units would account for only about 70% of the reaction progress observed in the WRF.

There are two possible explanations for the inability of dehydration reactions in the SPV and CGS to account for the reaction progress observed in the WRF in the Strafford syncline. The first possibility is that we have overestimated the amount of fluid infiltration required by underestimating the temperature of metamorphism. A higher temperature of metamorphism was suggested earlier for the Strafford syncline in the section on stable isotope systematics, but its validity relative to other explanations could not be determined. The second possibility is that there may have been an additional source of hydrous fluid for which we have not accounted, for instance, dehydration of the pelitic schists of the Gile Mountain Formation (GMF). The GMF is not as aluminous as the CGS, however, if it contains half as much modal garnet as the CGS contains, then the remaining 30% of the fluid required in the Strafford syncline can easily be derived from the GMF. With the dehydration of the pelites of the GMF as an additional source of fluids, fluid-present metamorphism of the WRF in the study area can be accounted for entirely by devolatilization of local units. There is no need for, and no evidence of, infiltration of exotic fluids.

This result differs from the findings of Ferry (1987) in the Waterville-Vassalboro area of Maine and the findings of Wickham and Taylor (1985) in the Trois Seigneurs Massif of France. Both of those studies concluded that regional-scale events of fluid infiltration had occurred during metamorphism of those areas. Both of these studies were conducted in rocks that were metamorphosed at shallower crustal levels (<15 km) than these rocks (~20 km). This might indicate that crustal scale fluid movement is less likely at deeper crustal levels, in agreement with Valley and O'Neil (1984). Alternatively, it may simply reflect the lack of a voluminous source of hydrous fluids in this location.

Acknowledgments

This work was supported by the Department of Earth Sciences at Dartmouth College, by grants from the Explorer's Club, Sigma Xi, and the Geological Society of America to D.B., and by National Science Foundation grants EAR-8957703 and EAR-8720160 and American Chemical Society grant PRF-19526-G2 to C.P.C. John B. Lyons read an earlier version of this paper. This paper benefited greatly from thoughtful and thorough reviews by Peter Nabelek, Steve Dunn, and John Brady.

References cited

Allen, T., and Chamberlain, C.P. (1989) Thermal consequences of mantled gneiss dome emplacement. Earth and Planetary Science Letters, 93, 392–404.

Baumgartner, L.P., and Rumble, D., III (1988) Transport of stable isotopes I: Development of a kinetic continuum theory for stable isotopic transport. Contributions to Mineralogy and Petrology, 98, 417–430.

Bence, A.E., and Albee, A.L. (1968) Empirical correction factors of the electron microanalysis of silicates and oxides. Journal of Geology, 76, 382–403.

Bottinga, Y. (1968) Calculation of fractionation factors for carbon and oxygen isotopic exchange in the system calcite-carbon dioxide-water. The Journal of Physical Chemistry, 27, 800–807.

Bottinga, Y., and Javoy, M. (1975) Oxygen isotope partitioning among the minerals in igneous and metamorphic rocks. Reviews of Geophysics and Space Physics, 13, 401–418.

Boxwell, M.A. (1986) Metamorphic history of the Standing Pond and Putney Volcanics in the Claremont, Bellows Falls and Saxtons River Quadrangles in southeastern Vermont. M.S. thesis, University of New Hampshire, Durham, New Hampshire.

Bragg, W.L. (1937) Atomic structure of minerals (1st edition). Cornell University Press, Ithaca, New York.

Bragg, W.L., and Claringbull, G.F. (1965) Crystal structure of minerals. G. Bell and Sons, London.

Broecker, W.S., and Oversby, V.M. (1971) Chemical equilibrium in the Earth. McGraw Hill, New York.

Chamberlain, C.P. (1986) Evidence for repeated folding of isotherms during regional metamorphism. Journal of Petrology, 27, 63–89.

Chamberlain, C.P., and Rumble, D., III (1988) Thermal anomalies in a regional metamorphic terrane: An isotopic study of the role of fluids. Journal of Petrology, 29, 1215–1232.

Chamberlain, C.P., Zeitler, P.K., and Jan, M.Q. (1989) The dynamics of the suture between the Kohistan Island arc and the Indian Plate in the Himalaya of Pakistan. Journal of Metamorphic Geology, 7, 135–149.

Chamberlain, C.P., Ferry, J.M., and Rumble, D., III (1990) The effect of net-transfer reactions on the isotopic composition of minerals. Contributions to Mineralogy and Petrology, 105, 322–336.

Clayton, R.N., and Maydea, T.K. (1963) The use of bromine penta-fluoride in the extraction of oxygen from oxides and silicates for isotopic analysis. Geochimica et Cosmochimica Acta, 27, 43–52.

Clayton, R.N., Goldsmith, J.R., and Mayeda, T.K. (1989) Oxygen isotope fractionation in quartz, albite, anorthite, and calcite. Geochimica et Cosmochimica Acta, 53, 725–733.

Doll, G.C. (1944) A preliminary report on the geology of the Strafford Quadrangle, Vermont. In G.C. Doll, Ed., Vermont State Geologists 24th biennial report, 1943–44, 14–28.

Duke, E.F., and Rumble, D., III (1986) Textural and isotopic variations in graphite from plutonic rocks. South Central New Hampshire. Contributions to Mineralogy and Petrology, 93, 409–419.

England, P., and Thompson, A.B. (1984) Pressure-temperature-time paths of regional metamorphism I. Heat transfer during the evolution of thickened continental crust. Journal of Petrology, 25, 894–928.

Ferry, J.M. (1983) Regional metamorphism of the Vasslboro Formation, South Central Maine, USA: A case study on the role of fluids in metamorphic petrogenesis. Journal of the Geological Society of London, 140, 551–576.

——— (1984) A biotite isograd in South-Central Maine, U.S.A.: Mineral reactions, fluid transfer and heat transfer. Journal of Petrology, 25, 871–893.

——— (1986) Reaction progress: A monitor of fluid-rock interaction. Advances in Physical Geochemistry, 5, 60–88.

——— (1987) Metamorphic hydrology at 13-km depth and 400–550 °C. American Mineralogist, 72, 39–58.

Ferry, J.M., and Burt, D.M (1982) Characterization of metamorphic fluid composition through mineral equilibria. Mineralogical Society of America Reviews in Mineralogy, 10, 207–262.

Fisher, G.W. (1980) Isograd migration in response to heat transfer during Acadian folding, Eastern Vermont. Geological Society of America Abstracts with Program, 426.

Friedman, I., and O'Neil, J.R. (1977) Compilation of isotopic fractionation factors of geochemical interest. U.S. Geological Survey Professional Paper 440-KK.

Graham, C.M., Greig, K.M., Sheppard, S.M.F., Turi, B. (1983) Genesis and mobility of the H_2O-CO_2 fluid phase greenschist metamorphism: A petrological and stable isotopic study in the Scottish Dalradian. Journal of the Geological Society of London, 140, 577–599.

Harker, R.I., and Tuttle, O.F. (1955) Studies in the system CaO, MgO, CO_2 part 2: Limits of the solid solution along the binary join $CaCO_3$, $MgCO_3$. American Journal of Science, 253, 274–282.

Hepburn, J.C., Trask, N.J., Rosenfeld, J.L., and Thompson, J.B., Jr. (1984) Bedrock geology of the Brattleboro Quadrangle, Vermont–New Hampshire. Vermont Geological Survey Bulletin 32, 162 p.

Hewitt, D.A. (1973) The metamorphism of micaceous limestones from south-central Connecticut. American Journal of Science, 273-A, 444–469.

Hoernes, S., and Hoffer, E. (1985) Stable isotopic evidence for fluid present and fluid absent metamorphism in metapelites from the Damara Orogen, Namibia. Contributions to Mineralogy and Petrology, 90, 322–330.

Hoisch, T.D. (1987) Heat transport by fluids during cretaceous regional metamorphism in the Big Maria Mountains, southeastern California. Geological Society of America Bulletin, 98, 549–553.

Howar, P.F. (1969) The geology of the Elizabeth Mine, Vermont. Vermont Geological Survey Economic Geology Bulletin 5.

Hueber, F.M., Bothner, W.A., Hatch, N.L., Finney, S.C., and Aleinikoff, J.N. (1990) Devonian plants from southern Quebec and northern New Hampshire and the age of the Connecticut Valley Trough. American Journal of Science, 290, 360–395.

Jacobs, G.K., and Kerrick, D.M. (1981) Methane: An equation of state with application to the ternary system H_2O-CO_2-CH_4. Geochimica et Cosmochimica Acta, 45, 607–614.

Kerrick, D.M., and Jacobs, G.K. (1981) A modified Redlich-Kwong equation for H_2O and CO_2 and H_2O-CO_2 mixtures at elevated pressures and temperatures. American Journal of Science, 281, 735–767.

Lux, D.R., DeYoreo, J.J., Guidotti, C.V., and Decker, E.R. (1986) Role of Plutonism in low-pressure metamorphic belt formation. Nature, 323, 794–796.

Lyons, J.B. (1955) Geology of the Hanover Quadrangle, New Hampshire–Vermont. Geological Society of America Bulletin, 66, 105–146.

Matsuhisa, Y., Goldsmith, J.R., and Clayton, R.N. (1979) Oxygen isotopic fractionation in the system in the system quartz-albite-anorthite-water. Geochimica et Cosmochimica Acta, 43, 1131–1140.

McCrea, J.M (1950) On the isotopic chemistry of carbonates and a paleotemperature scale. Journal of Chemical Physics, 18, 849–857.

Mohr, D.W. (1985) Fluid flow and alkalai transport within a metamorphic terrane, western North Carolina. Tectonophysics, 119, 329–348.

Nabelek, P.I. (1987) General equations for modeling fluid/rock interaction using trace elements and isotopes. Geochimica et Cosmochimica Acta, 51, 1765–1769.

Newton, R.C., and Haselton, H.T. (1981) Thermodynamics of the garnet-plagioclase-Al_2SiO_5-quartz geobarometer. Advances in Geochemistry, 1, 131–147.

Northrup, D.A., and Clayton, R.N. (1966) Oxygen isotope fractionations in systems containing dolomite. Journal of Geology, 74, 174–196.

Ohmoto, H., and Kerrick, D.M. (1977) Devolatilization equilibria in graphitic systems. American Journal of Science, 277, 1013–1044.

Rice, J.M., and Ferry, J.M. (1982) Buffering, infiltration, and the control of intensive variables during metamorphism. Mineralogical Society of America Reviews in Mineralogy, 10, 263–326.

Rosenfeld, J.L. (1968) Garnet rotations due to the major paleozoic deformations in South East Vermont. In E-an Zen, W.S. White, J.B. Hadley, and J.B. Thompson, Jr., Eds., Studies in appalachian geology, northern and maritime, p. 185–202. Wiley Interscience, New York.

Rumble, D., III, (1982) Stable isotopic fractionation during metamorphic devolatilization reactions. Mineralogical Society of America Reviews in Mineralogy, 10, 33–52.

Rumble, D., III and Hoering, T.C. (1986) Carbon isotope geochemistry of graphite vein deposits from New Hampshire, U.S.A. Geochimica et Cosmochimica Acta, 50, 1239–1247.

Rumble, D., III, Ferry, J.M., Hoering, T.C., and Boucot, A.J. (1982) Fluid flow during metamorphism at the Beaver Brook Fossil Locality, New Hampshire. American Journal of Science, 282, 886–919.

Ryzhenko, B.N., and Volkov, V.P. (1971) Fugacity coefficients of some gases in a broad range of temperatures and pressures. Geochemica International, 8, 468–481.

Selverstone, J., Spar, F.S., Franz, C., and Morteani, G. (1984) High pressure metamorphisms in the southwest Tauren Window, Austria: P-T paths from hornblende-kyanite-staurolite grabenschists. Journal of Petrology, 25, 501–531.

Sheppard, S.M.F., and Schwarcz, H.P. (1970) Fractionation of carbon and oxygen isotopes and magnesium between coexisting metamorphic calcite and dolomite. Contributions to Mineralogy and Petrology, 26, 161–198.

Sleep, N.H. (1979) A thermal constraint on the duration of folding with reference to Acadian geology, New England. Journal of Geology, 87, 583–589.

Spear, F.S., Hickmott, P., Crowley, P., and Hodges, K.V. (1984) P-T paths from garnet zoning: A new technique for deciphering tectonic processes in crystalline terranes. Geology, 12, 87–90.

Taylor, H.P., Jr. (1973) $^{18}O/^{16}O$ evidence for meteoric and hydrothermal alteration and ore deposition in the Tonopah, Comstock Lode, and gold field mining districts, Nevada. Economic Geology, 68, 747–764.

——— (1978) Oxygen and hydrogen isotope studies of plutonic granite rocks. Earth and Planetary Science Letters, 38, 177–210.

Taylor, H.P., Jr., Albee, A.L., and Epstein, S. (1963) $^{18}O/^{16}O$ ratios of coexisting minerals in three assemblages of kyanite zone peltic schist. Journal of Geology, 71, 513–522.

Thompson, J.B., Jr. (1979) The tschermak substitution and reactions in pelitic schists. In V.A. Zharikov, W.I. Fonarev, and S.P. Korikovskii, Eds., Problems in physiochemical petrology, vol. 1. Moscow Academy of Science, Moscow (in Russian).

——— (1981) An introduction to the mineralogy and petrology of the hydrous biopyriboles. Mineralogical Society of America Reviews in Mineralogy, 9A, 141–188.

——— (1982a) Composition space: An algebraic and geometric approach. Mineralogical Society of America Reviews in Mineralogy, 10, 1–32.

——— (1982b) Reaction space: An algebraic and geometric approach. Mineralogical Society of America Reviews in Mineralogy, 10, 33–52.

Thompson, J.B., Jr., Laird, J., and Thompson, A.B. (1982) Reaction in amphibolite, greenschist and blueschist. Journal of Petrology, 23, 1–27.

Tracy, R.J., Rye, D.M., Hewitt, D.A., and Schiffries, C.M. (1983) Petrologic and stable isotopic studies of fluid rock interaction, South Central Connecticut: I. The role of infiltration in producing reaction assemblages in impure marbles. American Journal of Science, 283A, 589–616.

Valley, J.W. (1986) Stable isotopic geochemistry of metamorphic rocks. Mineralogical Society of America Reviews in Mineralogy, 16, 445–489.

Valley, J.W., and O'Neil, J.R. (1984) Fluid heterogeneity during granulite facies metamorphism in the Adirondacks: Stable isotopic evidence. Contributions to Mineralogy and Petrology, 85, 158–173.

White, W.S., and Jahns, R.H. (1950) Structure of Central and East Central Vermont. Journal of Geology, 58, 179–220.

Wickham, S.M., and Taylor, H.P., Jr. (1985) Stable isotopic evidence for large scale seawater infiltration in a regional metamorphic terrane; the Trois Seigneurs Massif, Pyrennees, France. Contributions to Mineralogy and Petrology, 91, 122–137.

Manuscript received February 1, 1990
Manuscript accepted February 28, 1991